AGU PUBLICATIONS

Geochemistry, Geophysics, Geosystems

RESEARCH ARTICLE
10.1002/2016GC006419

Seismological structure of the 1.8 Ga Trans-Hudson Orogen of North America

Amy Gilligan[1], Ian D. Bastow[1], and Fiona A. Darbyshire[2]

[1]Department of Earth Science and Engineering, Imperial College London, London, UK, [2]Université du Québec à Montréal, Montréal, Québec, Canada

Key Points:
- First full crustal seismic models of the Trans-Hudson Orogen in northernmost Hudson Bay
- Proterozoic southern Baffin's crust is thicker, and its Moho more diffuse, than neighbouring Archean domains
- The Vs models for southern Baffin show similarities to the lower crust of Tibet

Supporting Information:
- Supporting Information S1
- Figure S1
- Figure S2

Correspondence to:
A. Gilligan,
a.gilligan@imperial.ac.uk

Citation:
Gilligan, A., I. D. Bastow, and F. A. Darbyshire (2016), Seismological structure of the 1.8 Ga Trans-Hudson Orogen of North America, *Geochem. Geophys. Geosyst.*, *17*, 2421–2433, doi:10.1002/2016GC006419.

Received 28 APR 2016
Accepted 31 MAY 2016
Accepted article online 3 JUN 2016
Published online 24 JUN 2016

Abstract Precambrian tectonic processes are debated: what was the nature and scale of orogenic events on the younger, hotter, and more ductile Earth? Northern Hudson Bay records the Paleoproterozoic collision between the Western Churchill and Superior plates—the ~1.8 Ga Trans-Hudson Orogeny (THO)—and is an ideal locality to study Precambrian tectonic structure. Integrated field, geochronological, and thermobarometric studies suggest that the THO was comparable to the present-day Himalayan-Karakoram-Tibet Orogen (HKTO). However, detailed understanding of the deep crustal architecture of the THO, and how it compares to that of the evolving HKTO, is lacking. The joint inversion of receiver functions and surface wave data provides new Moho depth estimates and shear velocity models for the crust and uppermost mantle of the THO. Most of the Archean crust is relatively thin (~39 km) and structurally simple, with a sharp Moho; upper-crustal wave speed variations are attributed to postformation events. However, the Quebec-Baffin segment of the THO has a deeper Moho (~45 km) and a more complex crustal structure. Observations show some similarity to recent models, computed using the same methods, of the HKTO crust. Based on Moho character, present-day crustal thickness, and metamorphic grade, we support the view that southern Baffin Island experienced thickening during the THO of a similar magnitude and width to present-day Tibet. Fast seismic velocities at >10 km below southern Baffin Island may be the result of partial eclogitization of the lower crust during the THO, as is currently thought to be happening in Tibet.

1. Introduction

1.1. Overview

The time period in Earth's history during which modern-style plate tectonic processes took over from the "vertical" plume [e.g., *Bédard*, 2006] and crustal delamination [e.g., *Zegers and van Keken*, 2001] processes that are often associated with the younger, hotter, more ductile Earth, is debated. Interpreting the Precambrian geological record in the context of processes occurring at present-day plate boundaries should therefore be carried out tentatively. Gathering structural information preserved in the plates deep beneath stable Precambrian regions (shields) using seismology can play an important role in our endeavours to understand the early Earth.

The geological record of northern Hudson Bay, Canada, spans >2 Ga of the Precambrian and is thus an ideal study locale for ancient tectonic processes. The region comprises several Archean cratons that assembled during a series of Paleoproterozoic collisions [e.g., *Hoffman*, 1988], culminating in the Trans-Hudson Orogeny (THO) ~1.8 Ga ago. Since the THO, the region has not experienced any significant tectonic activity. Much of our understanding of the THO comes from integrated field, geochronological and thermobarometric studies [e.g., *St-Onge et al.*, 2006; *Corrigan et al.*, 2009] and potential field maps [e.g., *Eaton and Darbyshire*, 2010]. On the strength of these data, *St-Onge et al.* [2006] proposed that the THO was an orogen of similar scale and nature to the present-day Himalayan-Karakoram-Tibet Orogen (HKTO) of Asia. Recent seismograph network deployments in the northern Hudson Bay region have provided fresh scope to analyze the THO [see e.g., *Bastow et al.*, 2015, for a review] and resulting studies have provided further support for earlier claims of similarities between the THO and HKTO [e.g., *Thompson et al.*, 2010; *Bastow et al.*, 2011; *Pawlak et al.*, 2011]. However, detailed absolute seismic wave speed constraints on the crustal and uppermost mantle architecture of the THO, and how these compare to the evolving HKTO, are presently lacking.

Using data from broadband seismograph stations across Archean cratons and zones involved in the Paleoproterozoic THO, we obtain the shear velocity structure for the Hudson Bay region through the joint

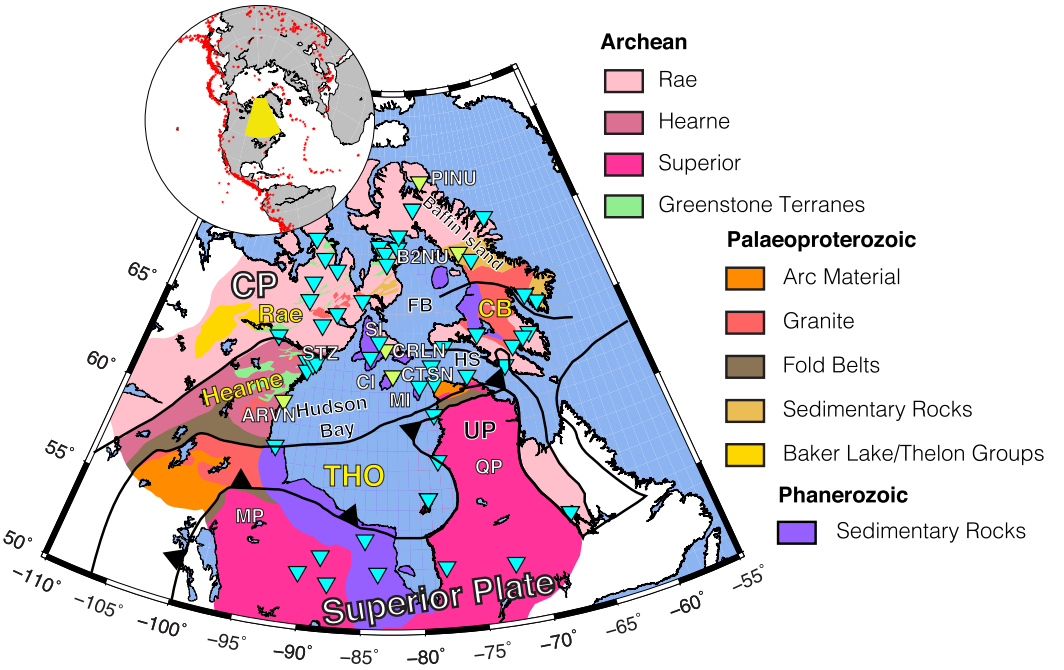

Figure 1. Geology of the Hudson Bay region. THO: Trans-Hudson Orogen, FB: Foxe Basin, SI: Southampton Island, CI: Coats Island, MI: Mansell Island, STZ: Snowbird Tectonic Zone, CP: Churchill Plate, CB: Cumberland Batholith, UP: Ungava Peninsula, HS: Hudson Strait, ChB: Chesterfield Block. Cyan and lime green triangles are seismograph station locations; green stations are those mentioned by name in the text. Inset: the locations of earthquakes used to calculate receiver functions (red stars). The yellow box marks the study area.

inversion of receiver function and surface wave data. This uses the same approach that *Gilligan et al.* [2015] applied to data from the western Himalayas and Tibet, which allows us to make the first detailed seismological comparison of the THO and the HKTO.

1.2. Tectonic Background and Previous Geophysical Studies

The crust of the Rae, Hearne, and Superior cratons (Figure 1) mainly formed during the Archean [e.g., *Hoffman*, 1988], with the oldest rocks found in these regions being up to 3.9 Ga in age [e.g., *Hartlaub et al.*, 2004, 2005; *van Breemen et al.*, 2007]. The Hudson Bay region also records evidence for the collisions involved in the formation of Laurentia, including the Trans-Hudson Orogeny (THO) [*Hoffman*, 1988], the best-preserved Paleoproterozoic orogenic belt on Earth.

The THO, which occurred 1.83–1.80 Ga ago [*Corrigan et al.*, 2009], was part of a series of collisions between Archean cratons, microcontinents, and island arc terranes in the early Paleoproterozoic. Earlier collisions saw the accretion of smaller continental blocks onto the margin of the Rae craton. These include the Hearne craton during the Snowbird Orogeny 1.91–1.89 Ga ago [*Berman et al.*, 2007], and the Meta Incognita microcontinent 1.883–1.865 Ga ago [*St-Onge et al.*, 2006]. The Rae and Hearne cratons, the Chesterfield block, and Meta Incognita together form the Western Churchill Plate [e.g., *Hoffman*, 1988]. The THO saw the collision between the Western Churchill and Superior plates leading to the formation of an orogenic belt, the THO, ~3000 km long stretching across cratonic North America [*Hoffman*, 1988]. The THO has been described as a double-indentor collision [e.g., *Gibb*, 1983]. The sinuous leading edge of the Superior plate results in a horseshoe shape to the orogen around Hudson Bay, with two promontories, the Quebec Promontory and the Manitoba Promontory, forming the two indentors (Figure 1).

Geological and geophysical work in the Hudson Bay region over the last decade has greatly increased our understanding of Precambrian processes [e.g., *Darbyshire*, 2003; *Bastow et al.*, 2011, 2015; *St-Onge et al.*, 2006; *Corrigan et al.*, 2009; *Snyder et al.*, 2013, 2015; *Pawlak et al.*, 2011, 2012; *Thompson et al.*, 2010, 2011; *Eaton and Darbyshire*, 2010; *Darbyshire and Eaton*, 2010; *Darbyshire et al.*, 2013; *Porritt et al.*, 2015]. In addition to addressing the timing of the onset of modern-day plate tectonics [*St-Onge et al.*, 2006; *Bastow et al.*, 2011], these studies have suggested that the collision between the Western Churchill and Superior plates

was more complex than a simple two-plate system: the presence of additional blocks, including the Sugluk block, has been inferred to have been involved in the collision [e.g., *Corrigan et al*., 2009].

Thompson et al. [2010] calculated P receiver functions for broadband seismograph stations around Hudson Bay, and used H-κ stacking [*Zhu and Kanamori*, 2000] to estimate bulk crustal Vp/Vs ratio and Moho depth variation across the region. They obtained Moho depths of between 34 and 43 km and, using their observations of age-dependent Vp/Vs ratios, concluded that the Hudson Bay region records the evolution of crustal formation processes from nonplate tectonics in the Paleoarchean to Mesoarchean, to plate tectonics by the Paleoproterozoic. *Snyder et al*. [2013, 2015] presented both radial and transverse receiver functions, migrated through an assumed velocity to depth. Their Moho depths agreed well with those of *Thompson et al*. [2010]. They argued, taken with other geophysical observations, including SKS splitting measurements, that the data show the presence of dipping layers in the upper mantle.

Our study is an advancement of the previous work of *Thompson et al*. [2010] in two main respects. First, we obtain a full shear velocity model, allowing for more detailed examination of the seismic structure of the crust and uppermost mantle than was afforded by their bulk-crustal study, which was inherently limited through the use of a H-κ stacking approach. We present, for the first time, an absolute shear velocity model for the crust in this region. Second, we use data from a larger number of stations (54 in this study, compared to 35 in *Thompson et al*. [2010]), in particular those located in the Superior region.

2. Data and Methods

Our teleseismic data were recorded at 54 broadband seismograph stations (Figure 1) around Hudson Bay from the POLARIS [*Eaton et al*., 2005], HuBLE-UK and CNSN networks. We calculated radial P receiver functions using the iterative deconvolution method of *Ligorría and Ammon* [1999] with a Gaussian parameter of 1.6, corresponding to a maximum frequency of 0.77 Hz.

We used 3566 high-quality receiver functions, selected from an initial set of 13,559, in our analysis. Quality control was performed on the receiver functions by comparing the original radial-component seismogram to the convolution between the vertical-component seismogram and the estimated receiver function. A fit of at least 70% was required to accept the receiver function for further analysis. Visual inspection of the remaining receiver functions for a given station removed those that were noisy, oscillatory or anomalous with respect to other receiver functions from a similar distance and backazimuth. For each station, all receiver functions were stacked to produce a single station trace with reduced noise. The total number of individual receiver functions (supporting information Table S1) at each station varied, dependent on how long the station was deployed. Several stations (e.g., Figure 4) exhibit systematic variations in the receiver functions with azimuth; we therefore also stacked receiver functions in narrow ($<30^{\circ}$) azimuthal bins to allow for further, more detailed investigation.

Receiver functions are sensitive to velocity discontinuities in the crust and mantle (e.g., the Moho) but with a strong trade-off between depth and Vp/Vs ratio and, consequently, depth and velocity [*Ammon et al*., 1990]. Jointly inverting receiver functions with surface wave dispersion data helps to reduce nonuniqueness because the dispersion data help to constrain absolute shear velocity at a site [*Özalaybey et al*., 1997].

We extracted 1-D fundamental mode Rayleigh wave group velocity dispersion curves from the GDM52 global compilation [*Ekstrom*, 2011] for each station location for a period range 25–250 s. This is the best group velocity data set available for this region that includes periods sensitive to both the crust and upper mantle, and includes data for the locations of all of the stations for which receiver functions are calculated. More detailed regional surface wave studies [e.g., *Darbyshire et al*., 2013; *Pawlak et al*., 2011, 2012] do exist; however, because of the distribution of seismograph stations, they are focused on Hudson Bay and do not have coverage to the north. It should be noted that the period range 25–250 s only constrains velocities in the lower crust and deeper: we are primarily using the surface wave data to ensure that the shear velocity values are realistic for this region to overcome the Vp/Vs-depth trade-off inherent in receiver function data.

Dispersion curves and radial P receiver function stacks for each station were inverted for shear velocity structure using *joint96* [*Herrmann*, 2013], an iterative linearized least squares inversion method. We used a starting model with a constant Vs = 4.48 km/s (as per the upper mantle velocity in the ak135 model of *Kennett et al*., [1995]) and Vp/Vs = 1.79 to 100 km depth, parameterized into 2 km thick layers, overlying

ak135 to 200 km depth. This is an approach used by previous studies using this method [e.g., *Rai et al*., 2006; *Acton et al*., 2011; *Gilligan et al*., 2015].Perturbing the starting model by ±0.2 km/s did not alter the resulting crustal structure, nor did lowering Vp/Vs to match the study of *Thompson et al*. [2010]. We also tested a significantly lower starting velocity of Vs = 3.7 km/s, typical of crustal velocities in this region (supporting information Figure S1). Using this starting model resulted in a velocity structure that was capable of fitting the receiver function data well, but the surface wave data at longer periods poorly: velocities in the upper mantle were too low, which could result in an underestimate of the absolute velocity change at the Moho, and thus different conclusions being made about the character of the Moho. Consequently, we prefer to use a starting model with higher velocities where the final model fits both the receiver function and surface wave data. Our starting model contains no a priori information about crustal thickness, so all crustal structure, such as the depth and velocity change at the Moho, is entirely data-driven. Inversions were run until they converged upon the best fitting mode. This is defined as being when the misfit reduction is less than 0.005%.

Joint inversions require choices of the relative weights attributed to each data type. In *joint96*, the relative weights for the receiver function and surface wave data are given by the *p* value, where the smaller the number, the greater the contribution from receiver functions. A *p* value of 0 means the inversion only includes receiver function data; a *p* value of 1 only includes surface wave data. We seek the model that has the maximum contribution from receiver functions but that maintains a good fit to the surface wave data, because the receiver functions have the greatest sensitivity to discontinuities such as the Moho. We tested *p* values of 0.5, 0.1, 0.05, 0.01, 0.001, and 0, and found that a value of 0.01 results in a good fit to both the receiver function and surface wave data. This small *p* value means that surface wave data have a small contribution to the final model in the inversion, and similar models result from inversions with no contributions from surface wave data. However, the inclusion of surface wave data allows us to directly constrain shear velocities in the lowermost crust and uppermost mantle. This then allows us to determine which, of a range of models that fit the receiver function data, best represents the Earth structure in this region, in particular the most appropriate upper mantle velocities and thus the velocity change at the Moho.

Receiver functions were also calculated for a Gaussian parameter of 2.5 and used in a joint inversion with surface wave data. Using these higher-frequency receiver functions was found to have no discernable impact on the results of the joint inversion; therefore, we describe only results where a Gaussian parameter of 1.6 was used in order to allow direct comparison with the results of *Gilligan et al*. [2015] from West Tibet.

3. Results

We obtain 1-D profiles of shear velocity versus depth at each station. These 1-D profiles are used to investigate variations in shear velocity throughout the region and to determine Moho depth and character. They are also combined into 2-D shear velocity cross sections to further investigate differences in crustal architecture between areas around Hudson Bay.

3.1. Shear Wave Velocity Structure

We group the velocity models into seven regions, (i) Rae, (ii) Hearne and Chesterfield, (iii) Northern Hudson Bay Islands, (iv) Superior, (v) Northeast Baffin Island, (vi) Southern Baffin Island, and (vii) Ungava, based on geographical location and previously documented lithospheric subdivisions (Figure 2). In the Rae domain, individual station velocity models are very similar to one another at most depths. In the uppermost crust, shear velocities are 3.3–3.6 km/s to ∼7 km depth, then 3.6–3.7 km/s to ∼30 km depth. Velocities then increase to ∼4.5 km/s between 30 and 38 km depth, at the seismological Moho.

The velocity structures obtained for stations in the Hearne and Chesterfield regions are similar and share many characteristics with the Rae domain (Figure 2). Uppermost crustal velocities, however, with the exception of station ARVN (Figure 1), are higher in the Hearne and Chesterfield (∼3.7 km/s) than in the Rae (∼3.4 km/s). Velocity structures for stations in the Superior craton are also similar to the Rae domain, but uppermost mantle velocities are higher.

Lower-crustal structure beneath the Northern Hudson Bay Islands is generally uniform between stations, and similar to that of the Rae and Hearne domains (Figure 2). The upper-crustal velocity structure (<20 km

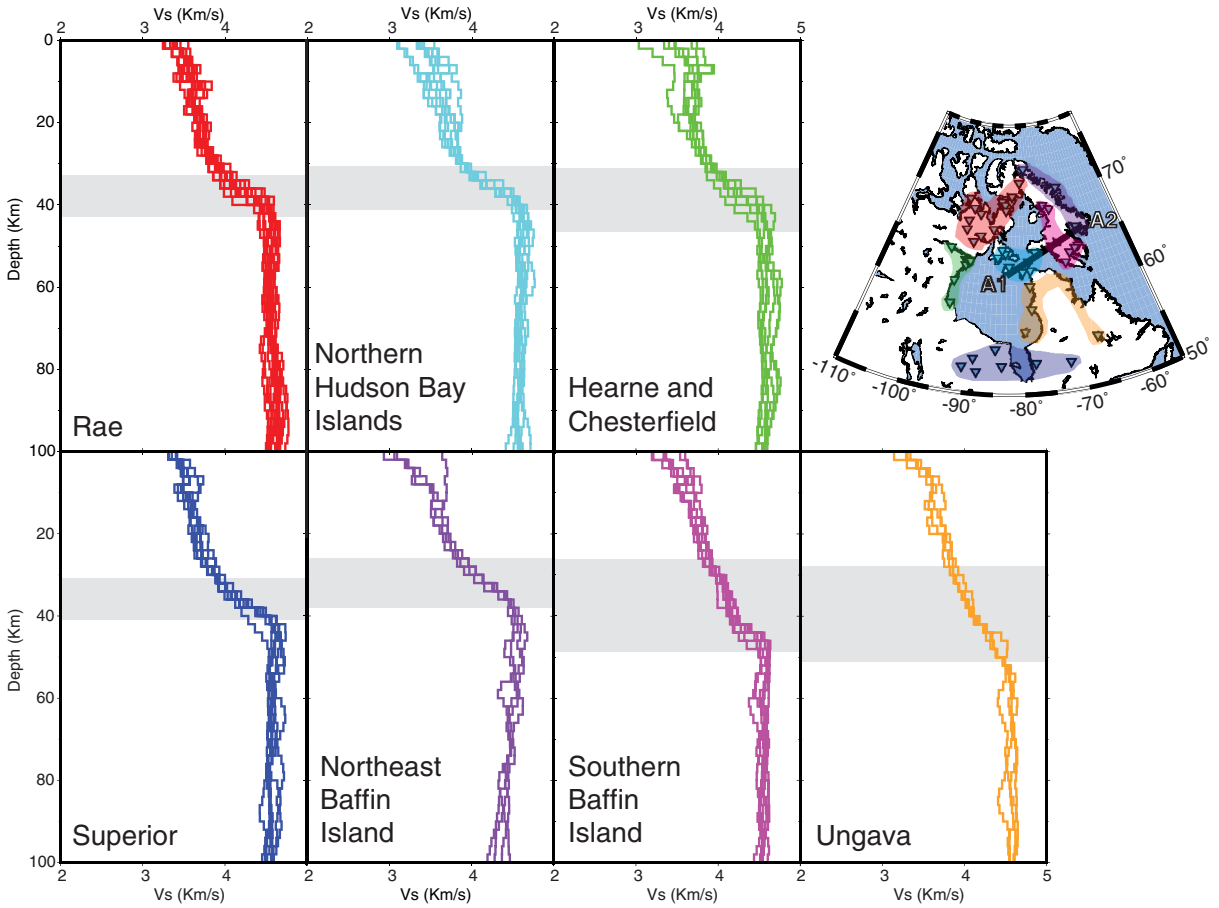

Figure 2. 1-D shear velocity profiles for each station from the joint inversion of P receiver functions and group velocity dispersion curves. The velocity profiles are grouped both geographically and seismologically on the basis of shear velocity structure and Moho character, and previously documented lithospheric subdivisions. The gray bands represent the depths over which velocities change from 3.8 to 4.5 km/s.

depth) is, however, more complex and variable. There is a wider range in velocities between stations (~3.0–3.6 km/s) than in other regions.

Receiver functions for stations CTSN and CRLN (Figure 3), located in the Northern Hudson Bay Islands region, show backazimuthal variation. In the case of CTSN, receiver functions from earthquakes with backazimuths to the south west have a large, positive amplitude P-to-S conversion at ~4 s, likely from the Moho. Those from the northwest have two lower amplitude, positive arrivals at 4.5 and 6.5 s, with the largest-amplitude arrival being a negative phase at ~8.5 s (Figure 3). As a result of this difference in receiver functions, velocity models from the joint inversion of stacked receiver functions from these two backazimuthal ranges are different. Forward modeling (Figure 4) demonstrates that velocity discontinuities in the upper crust and multiples from these discontinuities can explain the variations observed in the receiver functions. In the case of the receiver functions for station CTSN, from the NW the positive arrival at 4.5 s arises from the velocity increase associated with the Moho at ~38 km depth. The later positive (6.5 s) and negative arrivals (8.5 s) result from the multiples from a velocity increase in the upper crust at ~18 km depth (Figure 4). The azimuthal variation in the receiver functions may be due to the difference in the geology between the north and the south of the island: in the northern part, Precambrian basement rocks are exposed, while in the south, Phanerozoic sedimentary rocks are found at the surface.

On the northeastern edge of Baffin Island, three of the stations have low velocities in the upper 15 km of the crust: ~3 km/s at the surface, increasing to ~3.5 km/s by 15 km depth. For these stations, and station PINU, velocities increase to ~3.5–3.6 km/s by 25 km depth, then to ~4.5 km/s by a depth of ~35 km, a shallower depth than seen elsewhere.

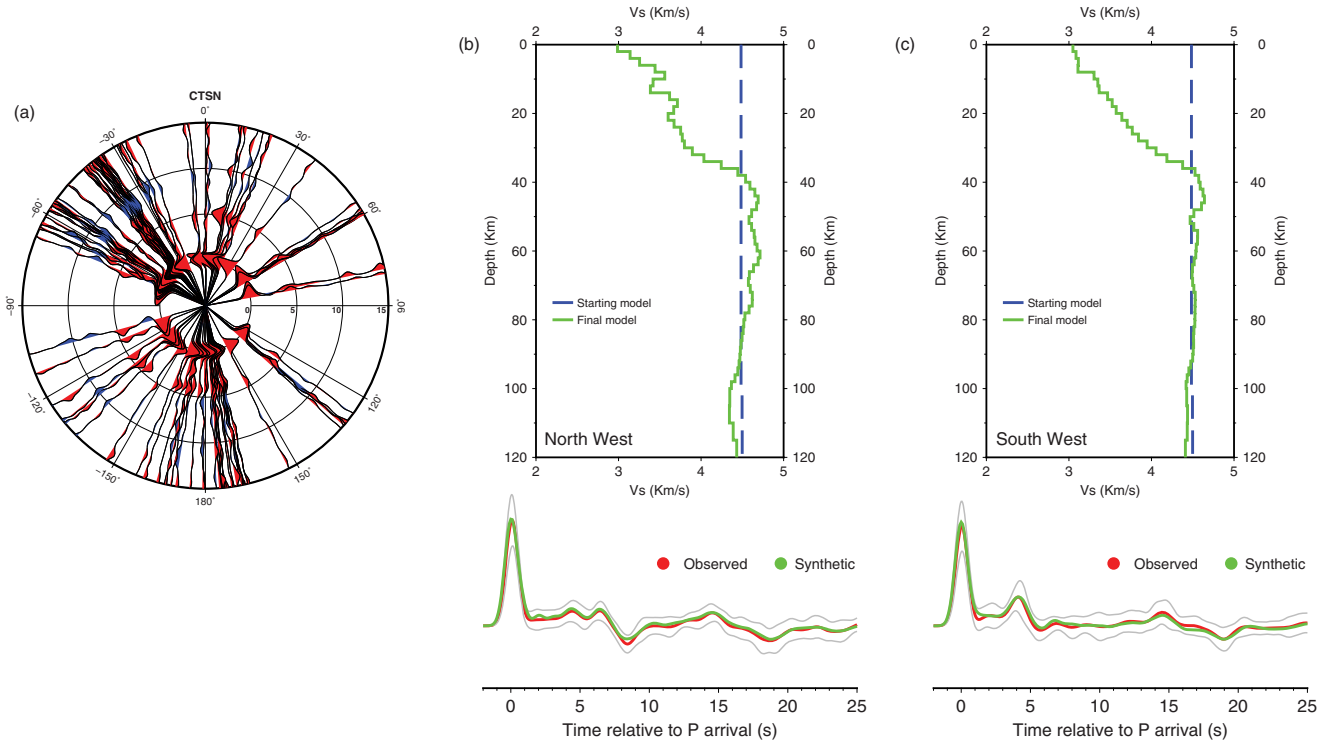

Figure 3. Individual radial P receiver functions from station CTSN (Coats Island) plotted by backazimuth. A clear difference can be seen between those in the northwest and in the southwest: in the SW there is an impulsive arrival at ~4.5 s, likely from the P-to-S conversion at the Moho, while receiver functions from earthquakes in the NW have lower amplitude, multiple positive peaks between 4 and 7 s, and a strong negative arrival at ~8.5 s. (a) Receiver functions from the NW are stacked into a single trace (red line, bottom), and jointly inverted with surface wave dispersion data to obtain a shear velocity model (top). The synthetic receiver function from this model (green line, bottom) shows a good match to the data. (b) As for (b), except for receiver functions from the SW. The shear velocity model shows a considerably simpler structure in the top ~25 km.

Southern Baffin Island exhibits relatively high upper-crustal velocities, increasing to ~3.7 km/s at 10 km depth and to ~4.2 km/s at 42 km depth, then to ~4.5 km/s at 46 km depth. Seismic crustal structure at stations on the Ungava peninsula shows a velocity increase from ~3.3 km/s in the uppermost crust to ~3.7–3.8 km/s at 5 km depth. There is then a gradual increase in velocity with depth to ~4.5 km/s at ~49 km depth. No abrupt change in velocity, representing the seismological Moho, is observed in the models for the Ungava peninsula.

3.2. Moho Depth and Character

Moho depth (Table 1, supporting information Table S1, and Figure 5) is picked from the 1-D shear velocity models (Figure 2) at the base of the steepest positive velocity gradient where Vs >4 km/s.

Throughout most of the Rae, Hearne and Chesterfield, Superior, and Northern Hudson Bay Islands, Moho depths are broadly similar (~34–42 km). On Baffin Island, the crust is thinner (~35 km) in the northeast than in the south, where the Moho depth reaches ~45 km.

Throughout most of the Archean regions, and on NE Baffin Island, the Moho is sharp, with the transition from crustal (~3.8 km/s) to mantle (≥4.5 km/s) velocities occurring over a ~2–5 km depth range. Accordingly, Moho P-to-S conversions are impulsive, large-amplitude arrivals in the receiver functions.

The Moho is more diffuse on southern Baffin Island (Figure 6a, Profile A1–A2). In the 1-D velocity profiles (Figure 2), where the gradient is steepest, there is a smaller velocity change than is seen in other regions: from ~4.2 to 4.5 km/s. The diffuse Moho on southern Baffin Island is also reflected in the P receiver functions, with the P-to-S conversion from the Moho being of lower amplitude.

Crustal thickness on the Ungava peninsula is difficult to determine from the velocity models since the 3.8–4.5 km/s transition is not abrupt. This is supported by the lower amplitude of the P-to-S conversions likely from the Moho in the receiver functions at stations. However, the depths at which velocities increase to

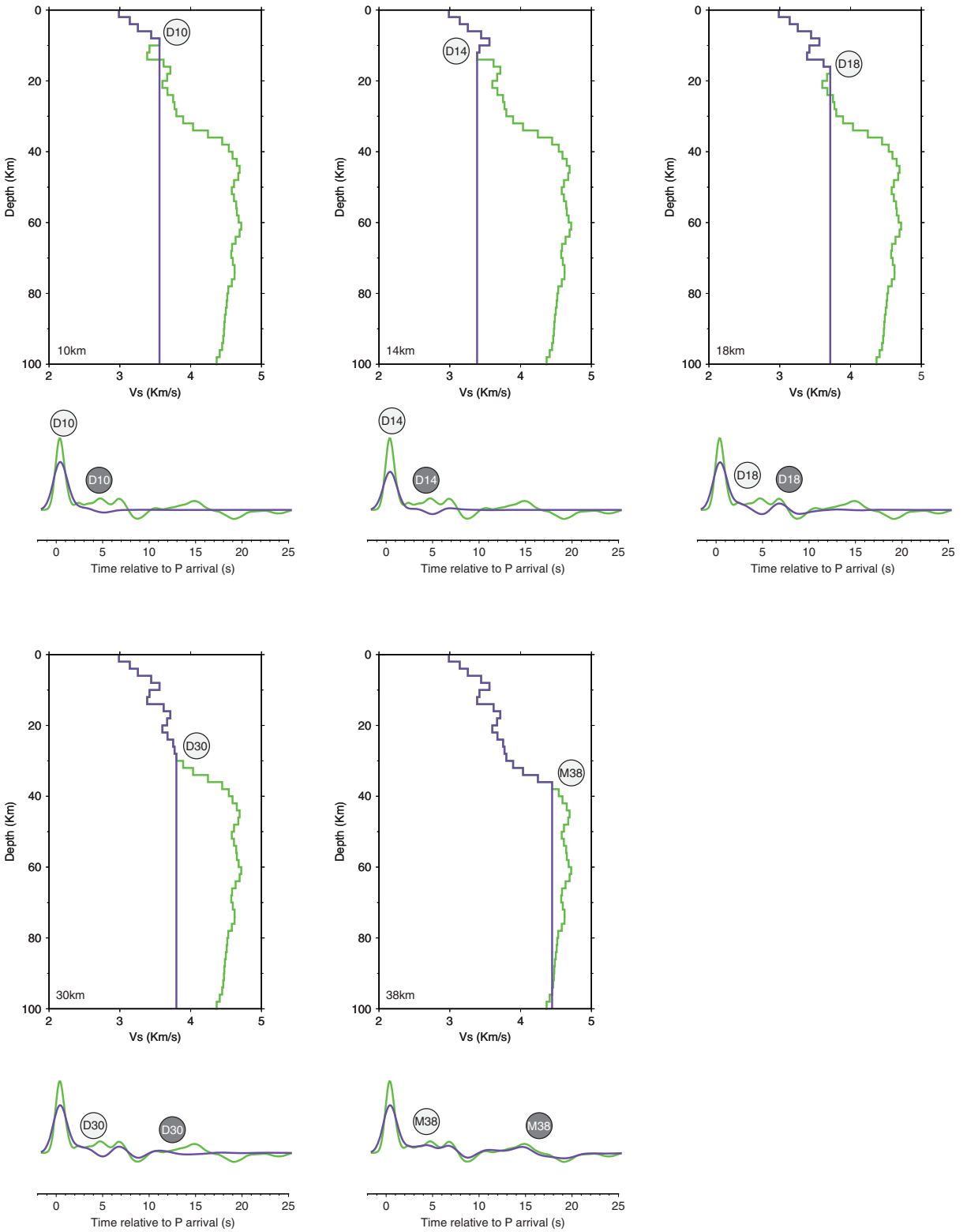

Figure 4. Velocity models and P receiver functions for station CTSN. The receiver function shown in purple is produced by the velocity model shown in purple for each of the plots. The green model and receiver function in each plot is the same, and are those which result from the joint inversion of stacked receiver functions from the north west from CTSN and surface wave dispersion measurements (i.e., Figure 3b). Each plot cuts the final model off at the depth indicated. The white circles label the velocity contrast of interest at that depth in the model plots and the time of P-to-S conversions from that discontinuity. The gray circles in the receiver function plots mark the time of the multiples from that discontinuity. The large negative arrival in the stacked receiver function is largely a result of multiples from a discontinuity at 18 km depth.

Table 1. Moho Depth and Character for Each of the Regions Shown in Figure 2[a]

Region	Number of Stations	Moho Depth Range (km)	Average Moho Depth (km)	Moho Character
Rae	15	36–42	39	Sharp
Islands	9	34–38	37	Sharp
Hearne and Chesterfield	7	36–42	39	Sharp
Superior	7	38–44	41	Sharp
NE Baffin	4	34–36	35	Sharp
Southern Baffin	7	44–50	45	Diffuse
Ungava	4	44–50	49	Diffuse

[a]Results for individual stations are shown in supporting information Table S2.

mantle velocities similar to those observed elsewhere in the Hudson Bay region are deeper than seen elsewhere in the other six areas (~49 km).

Our Moho depths agree well with those of *Thompson et al*. [2010] and *Darbyshire* [2003]. Where we have used stations not examined in previous studies, there is good consistency between neighboring stations. We do not find evidence in either the individual receiver functions or the shear velocity modeling for a layered Moho beneath some stations in the Rae and Chesterfield block as suggested by *Snyder et al*. [2015]. It is, however, possible that the frequency content of the receiver functions that we use prevents us from being able to resolve such layering.

4. Discussion

4.1. Archean Domains

Whether or not there is a large increase in shear velocities over a small depth range (<5 km) at the Moho can help to provide insight into processes of crustal formation and evolution. In general, the Archean regions (Rae, Hearne and Chesterfield, Northern Hudson Bay Islands, and Superior) have a relatively flat, sharp Moho at ~38–40 km depth. They have a simple crustal velocity structure: a small, gradual increase in velocities in the crust followed by a large increase of ~0.7 km/s at the Moho. This increase is even larger in the Superior, where the uppermost mantle is faster than elsewhere.

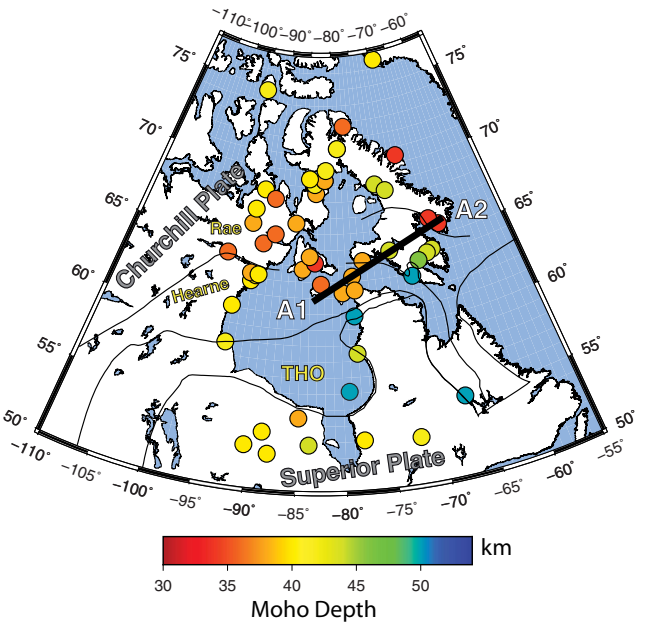

Figure 5. Moho depth variation around Hudson Bay and surroundings. Moho depths are picked from the 1D shear velocity models, obtained from the joint inversion of P receiver functions and surface wave dispersion curves, at the base of the steepest positive velocity gradient where Vs >4 km/s.

The similarity of Moho depth and seismic crustal and uppermost mantle structure across the Archean domains of northern Hudson Bay, across regions spanning over a thousand kilometers, implies that the processes that formed and subsequently shaped them may have been similar. Further, our results for Archean Canada are similar to those obtained via similar techniques for Africa and Arabia [e.g., *Kgaswane et al*., 2009; *Tugume et al*., 2013]. This supports proposals that crustal formation processes were similar throughout the Archean [e.g., *Tugume et al*., 2013].

Elevated lower-crustal temperatures (>650°C at the Moho; e.g., *Flament et al*. [2011]) in the Archean may have facilitated lower-crustal flow, leading to relatively uniform Moho depths, and prevented crustal thickening [e.g., *Rey and Houseman*, 2006]. Alternatively, *Thompson et al*. [2010] explained their H-κ stacking-derived observations of a

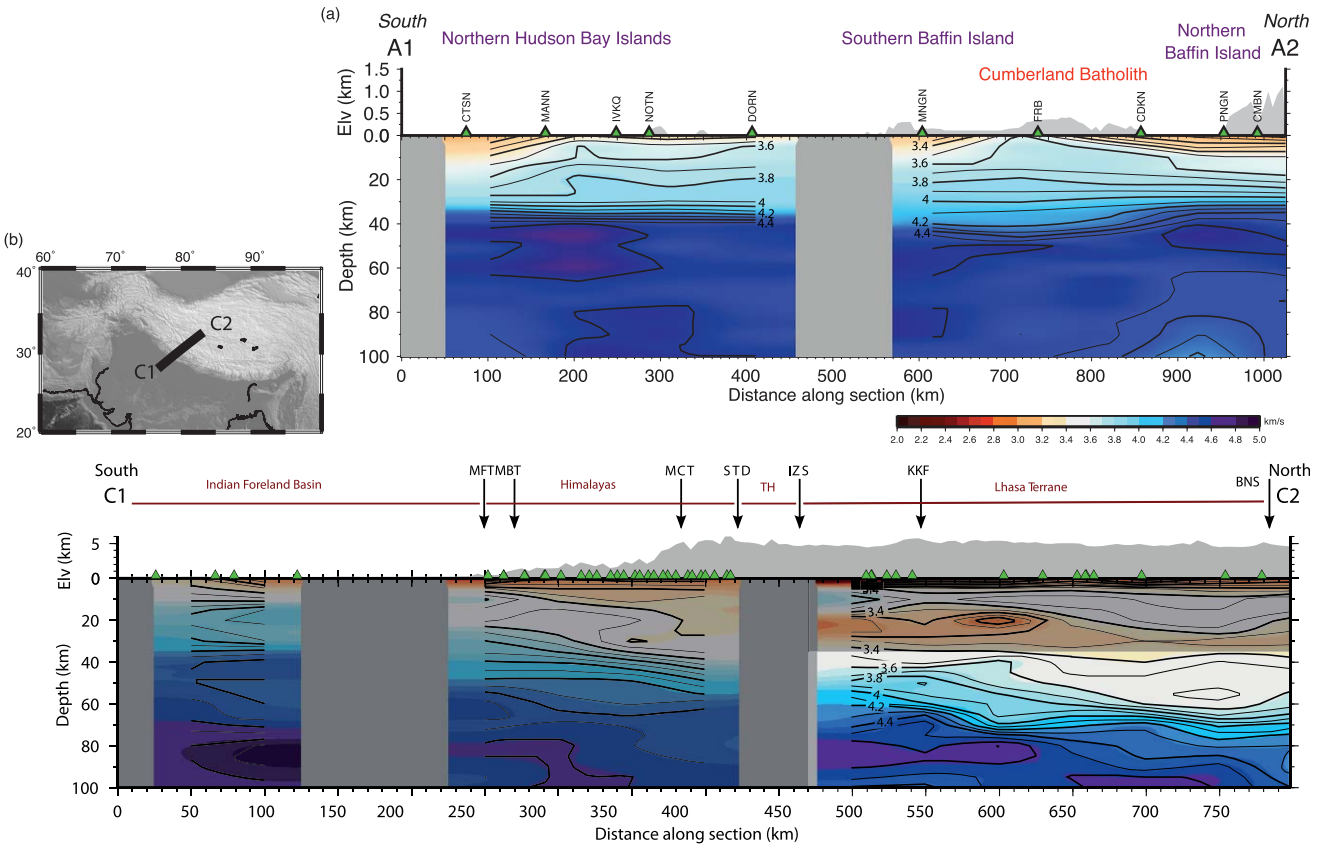

Figure 6. (a) Shear velocity cross section along the line A1–A2 (62°N, 83°W to 67°N, 65°W) from the joint inversion of P receiver functions and group velocity dispersion curves. The green triangles show the locations of stations. Gray regions are where there are gaps in station coverage. (a) Shear velocity cross section along the line C1-C2 (28.2°N, 76.7°E to 32.7°N, 83.2°E), shown in the inset map, modified from *Gilligan et al.* [2015]. The green triangles show the locations of stations. Gray regions are where there are gaps in station coverage. The lower crust beneath Tibet, which we consider comparable to the crust beneath southern Baffin Island, is highlighted, other regions are shaded.

sharp, flat Moho in the same region through the removal of restite by lower-crustal delamination following the formation of Tonalite-Trondhjemite-Granodiorite suites during the Archean. Petrological studies also support this hypothesis. *Abbott et al.* [2013], for example, suggest that the dense, garnet-rich, Archean lower crust readily delaminated because the lithospheric mantle was hotter and more ductile. This would produce a sharp, flat Moho and a more felsic crust. Accordingly, the shear velocities we obtain for the Archean cratons are characteristically felsic (3.6–3.7 km/s) [*Christensen*, 1996].

Elevated upper-crustal shear velocities in the Hearne domain, compared to the neighboring Rae, correlate with the presence of Archean greenstone belts (Figure 1). The crustal structure across the Snowbird Tectonic Zone (Figure 1), where the Rae and Hearne cratons sutured, is otherwise remarkably uniform. *Thompson et al.* [2010] found differences in the bulk crustal properties between the Rae and the Hearne, noting higher Vp/Vs in the Hearne than the Rae, which they suggested may reflect differences in how the crust was formed. *Jones et al.* [2002] also noted a difference between these two regions from magnetotelluric, SKS splitting, and receiver function results. However, we do not observe any notable differences in lower-crustal structure between the Rae, and Hearne and Chesterfield blocks (supporting information Figure S2). It may be that the H-κ results of *Thompson et al.* [2010], which only reflect bulk crustal structure, are strongly influenced by the relatively high velocities ($\sim$3.7 km/s) we observe in the uppermost crust of the Hearne and Chesterfield.

The uniform lower-crustal seismic structure throughout these regions suggests that evidence of deformation during the Snowbird Orogeny [*Berman et al.*, 2007] (e.g., crustal thickening, eclogitization of the lower crust) is not preserved. This may indicate that deformation did not affect the entirety of the crust, or that the Moho and lower-crustal velocity structure have been "reset" at some point since 1.91 Ga ago. The lower-crustal velocity structure may have potentially been reset due to the delamination of the lower crust as a result of eclogitization.

4.2. Trans-Hudson Orogen

The thickened crust and diffuse Moho on southern Baffin Island extends at least as far north as central Baffin Island to the Foxe Fold Belt (station B2NU). The seismic velocity structure here is distinct from surrounding regions in the Rae and Northern Hudson Bay Islands, where the crust is thinner and the Moho has a sharper velocity gradient: at the Moho velocities increase from 3.8 to 4.5 km/s over a smaller depth range than the change from the 4.2 to 4.5 km/s transition beneath southern Baffin. From geological observations, this area is known to have to have been deformed during the THO ~1.8 Ga ago [e.g., *Corrigan et al*., 2001; *St-Onge et al*., 2007], and has not experienced any orogenic activity since. The crustal thickening and diffuse Moho we observe are therefore likely to have resulted from processes occurring during the Trans-Hudson Orogen.

The seismic velocity structure and thinner crust beneath the Northern Hudson Bay Islands is very similar to that seen in the Rae, Hearne and Chesterfield, and Superior. This suggests that the crust here either did not experience deformation of the same style as on Southern Baffin Island during the THO, despite records of P-T conditions of 6.4–7.7 kbar and 630–790°C, 1.84–1.81 Ga ago on Southampton Island [*Berman et al*., 2011], or that the Moho has been reset at some point since the THO. The Moho may have been reset due to delamination following eclogitization of the lower crust, although *Corrigan et al*. [2009] suggest that the THO in the northern Hudson Bay region lacks the structural characteristics associated with orogenic collapse.

This difference in styles of deformation may be a result of differences in lithospheric thickness. Intriguingly, the thickest lithosphere (~280 km) beneath the Hudson Bay region is found beneath the Northern Hudson Bay Islands, thinning to ~180km beneath the Hudson Strait [*Darbyshire et al*., 2013]. *Darbyshire et al*. [2013] attributed the thinner lithosphere to Paleozoic extension. Alternatively, it may be that the relative difference in lithospheric thickness we observe today (thick beneath the islands, thinner beneath southern Baffin Island) is a long-lived feature and that thicker pre-THO lithosphere prevented deformation in these regions, and focused deformation on the southern Baffin Island region.

Shear velocity structures beneath the Ungava peninsula are unique within our study area: the crust-mantle transition is extremely gradational, with an increase from Vs ~3.8 to ~4.5 km/s occurring over a depth range of ~30 km, and the crust is thicker than elsewhere. All stations in the Ungava region, including those near the northern edge of the Superior craton, lie on crust that field geological studies infer to have been involved in the Trans-Hudson and New Quebec orogenies [e.g., *St-Onge et al*., 2006, 2000, Figure 1], as opposed to "typical" Superior craton crust.

The presence of Phanerozoic cover on Coats, Mansell, and the southern part of Southampton Island likely explains the lower upper-crustal velocities we observe there (Figure 2); lower-crustal velocities are comparatively uniform. Previous geological studies [e.g., *Corrigan et al.* 2009] have suggested the presence of a lithospheric block, the so-called Sugluk block, between the Rae and the Superior cratons, with a boundary between Southampton Island and Coats Island. A study of mantle seismic anisotropy by *Bastow et al*. [2011] found evidence for short length-scale variations in lithospheric structural fabrics across the same region. In contrast, our study of isotropic crustal shear velocity and Moho character yields no evidence in support for such a tectonic subdivision. Instead, a simple, two-block system can adequately explain the Quebec-Baffin segment of the THO.

4.3. A Comparison With Present-Day Tibet

The extent of thickened crust and diffuse Moho on southern Baffin Island implies a $\geq$650 km wide zone of deformation. This is a comparable spatial scale to the present-day Tibetan plateau, which ranges from 400 to 1000 km wide from west to east. *Gilligan et al*. [2015] used joint inversion of receiver functions and surface wave dispersion data to investigate crustal shear velocity structure of the western Himalayas and Tibet, providing an opportunity to compare the architecture of the modern-day HKTO and Paleoproterozoic THO.

Where we observe the thickest crust today correlates with the maximum pressure-temperature conditions on southern Baffin Island found by *St-Onge et al*. [2007]. They describe medium-pressure (6.3–9.8 kbar) and high-temperature metamorphism which, taking the average density for the crust in southern Baffin Island from the joint inversion results (~2950 kg/m^3), corresponds to depths of ~22–34 km. Density in the inversion is automatically calculated from the Vp/Vs ratio in the starting model of the joint inversion [*Herrmann*, 2013]. Using a lower, but plausible, density estimate only change the depth estimates by of tens of meters,

significantly lower than our depth resolution. Given the ~45 km thick crust beneath present-day southern Baffin Island and that the rocks now at the surface were once at 22–34 km depth, this suggests that crustal thickness during the THO would have been ~67–79 km, similar to that beneath present-day Tibet [65–85 km: e.g., *Gilligan et al*., 2015; *Bao et al*., 2015; *Acton et al*., 2011; *Nábělek et al*., 2009; *Schulte-Pelkum et al*., 2005; *Kind et al*., 2002]. These observations support the hypothesis that southern Baffin Island was an area of thickened crust, likely resulting in uplift and formation of a plateau similar to that in present-day Tibet.

The pressure-temperature conditions of the rocks at the surface on southern Baffin Island indicate that the upper crust has been removed since the THO. In Tibet today the upper to midcrust shows a number of features that may be important to the interpretation of tectonic processes that are occurring. This includes a midcrustal low-velocity zone at ~20–40 km depth [e.g., *Gilligan et al*., 2015; *Bao et al*., 2015; *Caldwell et al*., 2009; *Rapine et al*., 2003]. We would not necessarily expect to see such features in southern Baffin today because this material has been removed. As such, we focus on comparing the crustal structure of southern Baffin with that of the lower crust in Tibet.

The Moho in both regions is diffuse: beneath southern Baffin Island, the increase from 3.8 to 4.5 km/s occurs over a ~24 km depth range, while in western Tibet the increase occurs over a ~20 km depth range [*Gilligan et al*., 2015]. Further, lower-crustal shear velocities in western Tibet are similar to those observed throughout most of the crust on southern Baffin Island (Figure 4, >3.7 km/s). Eclogitization increases density and seismic velocity and will result in a diffuse crust-mantle transition. *Zhang et al*. [2014] argue that there is a 20 km thick, partially eclogitized layer at the base of the crust in West Tibet. Analogously, partial eclogitization may be responsible for the elevated velocities and diffuse Moho we observe in the crust beneath southern Baffin Island (Figure 2).

Eclogitized lower crust might be expected to have delaminated during orogenic collapse [e.g., *Nelson*, 1992], but the THO in the northern Hudson Bay region lacks the structural characteristics associated with orogenic collapse [*Corrigan et al*., 2009]. A partially eclogitized root may plausibly be preserved beneath southern Baffin Island. The preservation of a dense root over such an extended time period may indicate that only limited eclogitization occurred beneath southern Baffin Island, potentially due to low water content [*Leech*, 2001]. The sharp Moho we observe beneath the Northern Hudson Bay Islands may indicate that no partial eclogitization occurred in this region, potentially due to a lack of water. Subduction would deliver water into the upper mantle [e.g., *Garth and Rietbrock*, 2014]. The lack of observed partial eclogitization may imply that there was little subduction of the Superior plate beneath the islands, which would fit with there being a greater distance between the edge of the Superior plate and the northern Hudson Bay Islands than between the Superior plate and southern Baffin Island.

In the better-studied southwest portion of the THO it is suggested that in Manitoba and Saskatchewan the orogen did experience collapse [e.g., *Baird et al*., 1996,; *Schneider et al*., 2007], while in the US it did not [e.g., *Baird et al*., 1996]. The along-strike variability of the THO as observed today may result from the variations in the composition of the leading edge of the Superior plate. Along-strike variations in crustal and lithospheric seismic structure have been observed in Tibet [e.g., *Nunn et al*., 2014; *Agius and Lebedev*, 2013], and it may be that the HKTO will experience a similarly variable fate along-strike as the THO.

5. Conclusions

Through the joint inversion of receiver function and surface wave data, we have constrained the Moho character and depth, and, for the first time, crustal and uppermost mantle shear velocity structure for northernmost Hudson Bay, which includes a section of the ~1.8 Ga Trans-Hudson Orogen. Archean domains are structurally simple, with a ~39 km thick crust and sharp Moho. We find no direct evidence for lithospheric blocks (e.g., the Sugluk Block) caught up between the Churchill and Superior plates, nor do we find any evidence preserved of crustal thickening, of the scale we observe in modern-day orogens such as the HKTO, related to pre-THO collisions such as the Rae-Hearne. However, the crust is thicker and the Moho more diffuse beneath a region extending more than 650 km north from the Ungava Peninsula. These observations, when compared to velocity models derived for present-day Tibet, support the view that the THO was an orogen of similar scale to that observed in present-day Tibet. Further, it is likely that a partially eclogitized lower-crustal root, like that observed in Tibet today, has been preserved beneath southern Baffin Island

since the THO. Our results support previous geological and geophysical analyses that suggest that modern-style plate tectonics was in operation by Paleoproterozoic times.

Acknowledgments
Data for POLARIS stations were downloaded from the Canadian National Data Centre. POLARIS stations were funded by the Canadian Foundation for Innovation, Natural Resources Canada and Industry Canada. The HuBLE-UK (Hudson Bay Lithospheric Experiment) project was supported by Natural Environment Research Council (NERC) grant NE/F007337/1, with logistical support from the Geological Survey of Canada (GSC), Canada-Nunavut Geoscience Office (CNGO), SEIS-UK (the seismic node of NERC), and First Nations communities of Nunavut. This work was funded by Leverhulme Trust research project grant RPG-2013-332. F.D. is supported by NSERC through the Discovery Grants and Canada Research Chair programmes. We thank David Snyder for helpful comments on an earlier draft of this manuscript, and Leland O'Driscoll and an anonymous reviewer for feedback which helped to clarify several aspects of this manuscript. Figures were produced using Generic Mapping Tools [*Wessel et al.*, 2013].

References

Abbott, D. H., W. D. Mooney, and J. A. VanTongeren (2013), The character of the Moho and lower crust within Archean cratons and the tectonic implications, *Tectonophysics*, *609*, 690–705.

Acton, C. E., K. Priestley, S. Mitra, and V. K. Gaur (2011), Crustal structure of the Darjeeling—Sikkim Himalaya and southern Tibet, *Geophys. J. Int.*, *184*, 829–852.

Agius, M. R., and S. Lebedev (2013), Tibetan and Indian lithospheres in the upper mantle beneath Tibet: Evidence from broadband surface-wave dispersion, *Geochem. Geophys. Geosyst.*, *14*, 4260–4281, doi:10.1002/ggge.20274.

Ammon, C. J., G. E. Randall, and G. Zandt (1990), On the nonuniqueness of receiver function inversions, *J. Geophys. Res.*, *95*, 15,303–15,318.

Baird, D. J., K. D. Nelson, J. H. Knapp, J. J. Walters, and L. D. Brown (1996), Crustal structure and evolution of the Trans-Hudson orogen: Results from seismic reflection profiling, *Tectonics*, *15*(2), 416–426.

Bao X., X. Song, and J. Li (2015), High-resolution lithospheric structure beneath Mainland China from ambient noise and earthquake surface-wave tomography, *Earth Planet. Sci. Lett.*, *417*, 132–141.

Bastow, I. D., D. A. Thompson, J. Wookey, J. M. Kendall, G. Helffrich, D. B. Snyder, D. W. Eaton, and F. A. Darbyshire (2011), Precambrian plate tectonics: Seismic evidence from northern Hudson Bay, Canada, *Geology*, *39*, 91–94.

Bastow, I. D., D. W. Eaton, J. M. Kendall, G. Helffrich, D. B. Snyder, D. A. Thompson, J. Wookey, F. A. Darbyshire, and A. E. Pawlak (2015), The Hudson Bay Lithospheric Experiment (HuBLE): Insights into Precambrian plate tectonics and the development of mantle keels, in *Continent Formation Through Time*, vol. 389, edited by N. M. W. Roberts et al., pp. 41–67, Geol. Soc. Spec. Publ., London, U. K.

Bédard, J. H. (2006), A catalytic delamination-driven model for coupled genesis of Archaean crust and sub-continental lithospheric mantle, *Geochim. Cosmochim. Acta*, *70*, 1188–1214.

Berman, R. G., W. J. Davis, and S. Pehrsson (2007), Collisional Snowbird tectonic zone resurrected: Growth of Laurentia during the 1.9 Ga accretionary phase of the Hudsonian orogeny, *Geology*, *35*, 911–914.

Berman, R.G., N. Rayner, M. Sanborn-Barrie, and J. Chakungal (2011), New constraints on the tectonothermal history of Southampton Island, Nunavut, provided by in situ SHRIMP geochronology and thermobarometry, *Geol. Surv. Can. Curr. Res. Pap.*, *2011-6*, 14 pp., doi:10.4095/287287.

Caldwell, W. B., S. L. Klemperer, S. S. Rai, and J. F. Lawrence (2009), Partial melt in the upper-middle crust of the northwest Himalaya revealed by Rayleigh wave dispersion, *Tectonophysics*, *477*, 58–65.

Christensen, N. I. (1996), Poisson's ratio and crustal seismology, *J. Geophys. Res.*, *101*, 3139–3156.

Corrigan, D., D. J. Scott, and M. R. St-Onge (2001), Geology of the northern margin of the Trans-Hudson Orogen (Foxe fold belt), central Baffin Island, Nunavut, *Geol. Surv. Can. Curr. Res. Pap. C*, *23*, 1–15.

Corrigan, D., S. Pehrsson, N. Wodicka, and E. De Kemp (2009), The Palaeoproterozoic Trans-Hudson Orogen: A prototype of modern accretionary processes, in *Ancient Orogens and Modern Analogues*, vol. 327, edited by J. B. Murphy, J. D. Keppie and A. J. Hynes, pp. 457–479, Geol. Soc. Spec. Publ., London, U. K.

Darbyshire, F. A. (2003), Crustal structure across the Canadian High Arctic region from teleseismic receiver function analysis, *Geophys. J. Int.*, *152*, 372–391.

Darbyshire, F. A., and D. W. Eaton (2010), The lithospheric root beneath Hudson Bay, Canada from Rayleigh wave dispersion: No clear seismological distinction between Archean and Proterozoic mantle, *Lithos*, *120*, 144–159.

Darbyshire, F. A., D. W. Eaton, and I. D. Bastow (2013), Seismic imaging of the lithosphere beneath Hudson Bay: Episodic growth of the Laurentian mantle keel, *Earth Planet. Sci. Lett.*, *373*, 179–193.

Eaton, D. W., and F. Darbyshire (2010), Lithospheric architecture and tectonic evolution of the Hudson Bay region, *Tectonophysics*, *480*, 1–22.

Eaton, D. W., J. Adams, I. Asudeh, G. M. Atkinson, M. G. Bostock, J. F. Cassidy, I. Ferguson, C. Samson, D. Snyder, K. F. Tiampo, et al. (2005), Investigating Canada's lithosphere and earthquake hazards with portable arrays. *Eos Trans. AGU*, *86*(17), 169–173.

Ekström, G. (2011), A global model of Love and Rayleigh surface wave dispersion and anisotropy, 25–250 *s, Geophys. J. Int.*, *187*, 1668–1686.

Flament, N., P. F. Rey, N. Coltice, G. Dromart, and N. Olivier (2011), Lower crustal flow kept Archean continental flood basalts at sea level, *Geology*, *39*, 1159–1162.

Garth, T., and A. Rietbrock (2014), Order of magnitude increase in subducted H_2O due to hydrated normal faults within the Wadati-Benioff zone, *Geology*, *42*, 207–210.

Gibb, R. A. (1983), Model for suturing of Superior and Churchill plates: An example of double indentation tectonics, *Geology*, *11*, 413–417.

Gilligan, A., K. F. Priestley, S. W. Roecker, V. Levin, and S. S. Rai (2015), The crustal structure of the western Himalayas and Tibet, *J. Geophys. Res.*, *120*, 3946–3964, doi:10.1002/2015JB011891.

Hartlaub, R. P., L. M. Heaman, K. E. Ashton, and T. Chacko (2004), The Archean Murmac Bay Group: Evidence for a giant Archean rift in the Rae Province, Canada, *Precambrian Res.*, *131*, 345–372.

Hartlaub, R. P., T. Chacko, L. M. Heaman, R. A. Creaser, K. E. Ashton, and A. Simonetti (2005), Ancient (Meso-to Paleoarchean) crust in the Rae Province, Canada: Evidence from Sm–Nd and U–Pb constraints, *Precambrian Res.*, *141*, 137–153.

Herrmann, R. B. (2013), Computer programs in seismology: An evolving tool for instruction and research, *Seismol. Res. Lett.*, *84*, 1081–1088, doi:10.1785/0220110096.

Hoffman, P. F. (1988), United Plates of America, the birth of a craton—Early Proterozoic assembly and growth of Laurentia, *Ann. Rev. Earth Planet. Sci.*, *16*, 543–603.

Jones, A. G., D. Snyder, S. Hanmer, I. Asudeh, D. White, D. Eaton, and G. Clarke (2002), Magnetotelluric and teleseismic study across the Snowbird Tectonic Zone, Canadian Shield: A Neoarchean mantle suture?, *Geophys. Res. Lett.*, *29*(17), 1829, doi:10.1029/2002GL015359.

Kgaswane, E. M., A. A. Nyblade, J. Julia, P. H. Dirks, R. J. Durrheim, and M. E. Pasyanos (2009), Shear wave velocity structure of the lower crust in southern Africa: Evidence for compositional heterogeneity within Archaean and Proterozoic terrains, *J. Geophys. Res.*, *114*, B12304, doi:10.1029/2008JB006217.

Kennett, B. L. N., E. R. Engdahl, and R. Buland (1995), Constraints on seismic velocities in the Earth from traveltimes, *Geophys. J. Int.*, *122*, 108–124.

Kind, R., X. Yuan, J. Saul, D. Nelson, S. V. Sobolev, J. Mechie, W. Zhao, G. Kosarev, J. Ni, U. Achauer, et al. (2002), Seismic images of crust and upper mantle beneath Tibet: Evidence for Eurasian plate subduction, *Science*, *298*, 1219–1221.

Leech, M. L. (2001), Arrested orogenic development: Eclogitization, delamination, and tectonic collapse, *Earth Planet. Sci. Lett.*, *185*, 149–159.

Ligorría, J. P., and C. J. Ammon (1999), Iterative deconvolution and receiver-function estimation, *Bull. Seismol. Soc. Am.*, *89*, 1395–1400.

Nábělek, J., G. Hetényi, J. Vergne, S. Sapkota, B. Kafle, M. Jiang, H. Su, J. Chen, B. S. Huang, and the Hi-CLIMB Team (2009), Underplating in the Himalaya-Tibet collision zone revealed by the Hi-CLIMB experiment, *Science*, *325*, 1371–1374.

Nelson, K. D. (1992), Are crustal thickness variations in old mountain belts like the Appalachians a consequence of lithospheric delamination?, *Geology*, *20*, 498–502.

Nunn, C., S. W. Roecker, K. F. Priestley, X. Liang, and A. Gilligan (2014), Joint inversion of surface waves and teleseismic body waves across the Tibetan collision zone: The fate of subducted Indian lithosphere, *Geophys. J. Int.*, *198*, 1526–1542.

Özalaybey, S., M. K. Savage, A. F. Sheehan, J. N. Louie, and J. N. Brune (1997), Shear-wave velocity structure in the northern Basin and Range province from the combined analysis of receiver functions and surface waves, *Bull. Seismol. Soc. Am.*, *87*, 183–199.

Pawlak, A., D. W. Eaton, I. D. Bastow, J. M. Kendall, G. Helffrich, J. Wookey, and D. Snyder (2011), Crustal structure beneath Hudson Bay from ambient-noise tomography: Implications for basin formation, *Geophys. J. Int.*, *184*, 65–82.

Pawlak, A., D. W. Eaton, F. Darbyshire, S. Lebedev, and I. D. Bastow (2012), Crustal anisotropy beneath Hudson Bay from ambient noise tomography: Evidence for post-orogenic lower-crustal flow?, *J. Geophys. Res.*, *117*, B08301, doi:10.1029/2011JB009066.

Porritt, R. W., M. S. Miller, and F. A. Darbyshire (2015), Lithospheric architecture beneath Hudson Bay, *Geochem. Geophys. Geosyst.*, *16*, 2262–2275, doi:10.1002/2015GC005845.

Rai, S., K. Priestley, V. Gaur, S. Mitra, M. Singh, and M. Searle (2006), Configuration of the Indian Moho beneath the NW Himalaya and Ladakh, *Geophys. Res. Lett.*, *33*, L15308, doi:10.1029/2006GL026076.

Rapine, R., F. Tilmann, M. West, J. Ni, and A. Rodgers (2003), Crustal structure of northern and southern Tibet from surface wave dispersion analysis, *J. Geophys. Res.*, *108*(B2), 2120, doi:10.1029/2001JB000445.

Rey, P. F., and G. Houseman (2006), Lithospheric scale gravitational flow: The impact of body forces on orogenic processes from Archaean to Phanerozoic, in *Analogue and Numerical Modelling of Crustal-Scale Processes*, vol. 253, No. 1, edited by S. J. H. Buiter and G. Schreurs, pp. 153–167, Geol. Soc. Spec. Publ., London, U. K.

Schneider, D. A., M. T. Heizler, M. E. Bickford, G. L. Wortman, K. C. Condie, and S. Perilli (2007), Timing constraints of orogeny to cratonization: Thermochronology of the Paleoproterozoic Trans-Hudson orogen, Manitoba and Saskatchewan, Canada, *Precambrian Res.*, *153*, 65–95.

Schulte-Pelkum, V., G. Monsalve, A. Sheehan, M. R. Pandey, S. Sapkota, R. Bilham, and F. Wu (2005), Imaging the Indian subcontinent beneath the Himalaya, *Nature*, *435*, 1222–1225.

Snyder, D. B., R. G. Berman, J. M. Kendall, and M. Sanborn-Barrie (2013), Seismic anisotropy and mantle structure of the Rae craton, central Canada, from joint interpretation of SKS splitting and receiver functions, *Precambrian Res.*, *232*, 189–208.

Snyder, D. B., J. A. Craven, M. Pilkington, and M. J. Hillier (2015), The 3-dimensional construction of the Rae craton, central Canada, *Geochem. Geophys. Geosyst.*, *16*, 3555–3574, doi:10.1002/2015GC005957.

St-Onge, M. R., N. Wodicka, and S. B. Lucas (2000) Granulite-and amphibolite-facies metamorphism in a convergent-plate-margin setting: Synthesis of the Quebec–Baffin segment of the Trans-Hudson orogeny, *Can. Mineral.*, *38*, 379–398.

St-Onge, M. R., M. P. Searle, and N. Wodicka (2006), Trans-Hudson Orogen of North America and Himalaya-Karakoram-Tibetan Orogen of Asia: Structural and thermal characteristics of the lower and upper plates, *Tectonics*, *25*, TC4006, doi:10.1029/2005TC001907.

St-Onge, M. R., N. Wodicka, and O. Ijewliw (2007), Polymetamorphic evolution of the Trans-Hudson Orogen, Baffin Island, Canada: Integration of petrological, structural and geochronological data, *J. Petrol.*, *48*, 271–302.

Thompson, D. A., I. D. Bastow, G. Helffrich, J. M. Kendall, J. Wookey, D. B. Snyder, and D. W. Eaton (2010), Precambrian crustal evolution: Seismic constraints from the Canadian Shield, *Earth Planet. Sci. Lett.*, *297*, 655–666.

Thompson, D. A., G. Helffrich, I. D. Bastow, J. M. Kendall, J. Wookey, D. W. Eaton, and D. B. Snyder (2011), Implications of a simple mantle transition zone beneath cratonic North America, *Earth Planet. Sci. Lett.*, *312*(1), 28–36.

Tugume, F., A. Nyblade, J. Julià, and M. van der Meijde (2013), Crustal shear wave velocity structure and thickness for Archean and Proterozoic terranes in Africa from modeling receiver functions, surface wave dispersion, and satellite gravity data, *Tectonophysics*, *609*, 250–266.

van Breemen, O., C. T. Harper, R. G. Berman, and N. Wodicka (2007), Crustal evolution and Neoarchean assembly of the central–southern Hearne domains: Evidence from U–Pb geochronology and Sm–Nd isotopes of the Phelps Lake area, northeastern Saskatchewan, *Precambrian Res.*, *159*, 33–59.

Wessel, P., W. H. F. Smith, R. Scharroo, J. F. Luis, and F. Wobbe (2013), Generic Mapping Tools: Improved version released, *EOS Trans, AGU*, *94*, 409–410.

Zegers, T. E., and P. E. van Keken (2001), Middle Archean continent formation by crustal delamination, *Geology*, *29*, 1083–1086.

Zhang, Z., Y. Wang, G. A. Houseman, T. Xu, Z. Wu, X. Yuan, Y. Chen, X. Tian, Z. Bai, and J. Teng (2014), The Moho beneath western Tibet: Shear zones and eclogitization in the lower crust, *Earth Planet. Sci. Lett.*, *408*, 370–377.

Zhu, L., and H. Kanamori (2000), Moho depth variation in southern California from teleseismic receiver functions, *J. Geophys. Res.*, *105*, 2969–2980, doi:10.1016/S0012-821X(00)00101-1.